REPORT DOCUMENTATION PAGE

Form Approved
OMB NO. 0704-0188

1. AGENCY USE ONLY (Leave Blank)	2. REPORT DATE 1/6/2003	3. REPORT TYPE AND DATES COVERED Final Progress Report 4/16/2001-11/30/2002

4. TITLE AND SUBTITLE
Biomolecular Recognition of Semiconductors and Magnetic Materials to Assemble Nanoparticle Heterostructures

5. FUNDING NUMBERS
C - DAAD19-01-1-0456

6. AUTHOR(S)
Belcher, Angela M.

7. PERFORMING ORGANIZATION NAME(S) AND ADDRESS(ES)
The University of Texas at Austin
Office of Sponsored Projects, Campus Mail Code: F3900
Austin, TX 78712

8. PERFORMING ORGANIZATION REPORT NUMBER

9. SPONSORING / MONITORING AGENCY NAME(S) AND ADDRESS(ES)
U. S. Army Research Office
P.O. Box 12211
Research Triangle Park, NC 27709-2211

10. SPONSORING / MONITORING AGENCY REPORT NUMBER
41358.2-LS-YIP

11. SUPPLEMENTARY NOTES
The views, opinions and/or findings contained in this report are those of the author(s) and should not be construed as an official Department of the Army position, policy or decision, unless so designated by other documentation.

12 a. DISTRIBUTION / AVAILABILITY STATEMENT
Approved for public release; distribution unlimited.

12 b. DISTRIBUTION CODE

13. ABSTRACT (Maximum 200 words)

We have focused on selecting peptides to control the synthesis of semiconductor and magnetic materials and extended it to multi-dimensional architectures. We have shown that a single phage selected for ZnS has a binding site (pIII) on one end of the phage that can nucleate and bind up to 5 ZnS nanoparticles. We took the clones that bind to ZnS nanocrystals through the pIII minor coat protein and cloned them into the pVIII major coat protein of the phage. There are 2700 copies of the pVIII protein that self- assemble to make the liner structure of the phage. More importantly, these pVIII proteins are all crystallographically related to each other. So cloning ZnS specific peptides into the crystalline coat allows us to lock in a particular orientation of the peptide on the coat and therefore translate the symmetry of the phage coat to a nucleated nanoparticle. We have used this clone to grow orientated ZnS nanoparticles along the "backbone" of the phage to make phage ZnS hybrid nanowires. Phage were also used to grow and assemble 2-6 semiconductors, gold nanoparticles and fluorescent molecules into highly ordered liquid crystalline phases and crystalline thin films.

14. SUBJECT TERMS nanomaterial, phage, self-assembly, quantum dots, liquid crystals, phage display	15. NUMBER OF PAGES 13
	16. PRICE CODE

17. SECURITY CLASSIFICATION OR REPORT	18. SECURITY CLASSIFICATION ON THIS PAGE	19. SECURITY CLASSIFICATION OF ABSTRACT	20. LIMITATION OF ABSTRACT
UNCLASSIFIED	UNCLASSIFIED	UNCLASSIFIED	UL

Angela M.Belcher
Final report on ARO PECASE DAAD 19-01-1-0456
For transfer of grant from University of Texas to MIT

Table of Contents **pgs**

PECASE ARO GRANT Final for Transfer to MIT

Angela M. Belcher The University of Texas at Austin

2. (4). Problem : We have focused on selecting peptides to control the synthesis of semiconductor and magnetic materiasl and extended it to multi-dimensional architectures.

2. (5). Summary of Important Results:

Phage grow nanoparicles/virus based nanowires

We have shown that a single phage selected for ZnS has a binding site (pIII) on the one end of the phage that can nucleate and bind up to 5 ZnSnanoparticles.

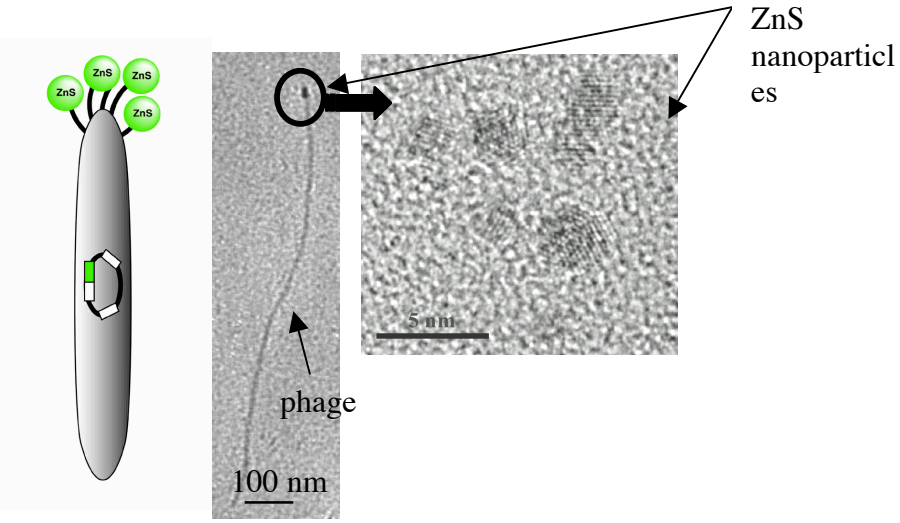

Figure 1 **(A)** **(B)**

We are now taking the clones that are shown to bind ZnS nanocrystals through the pIII minor coat protein (as shown above) and clone them into the pVIII major coat protein of the phage. There are 2700 copies of the pVIII protein that self- assemble to make the liner structure of the phage. More importantly, these pVIII proteins are all crystallographically related to each other. So cloning ZnS specific peptides into the crystalline coat allows us to lock in a particular orientation of the peptide on the coat and therefore translate the symmetry of the phage coat to a nucleated nanoparticle. Initial data suggest that can clone and express a ZnS specific particle on the major coat of the phage. We have used this clone to grow orientated ZnS nanoparticles along the “backbone” of the phage to make phage ZnS hybrid nanowires (Figure 2 and 3, In review for Nature).

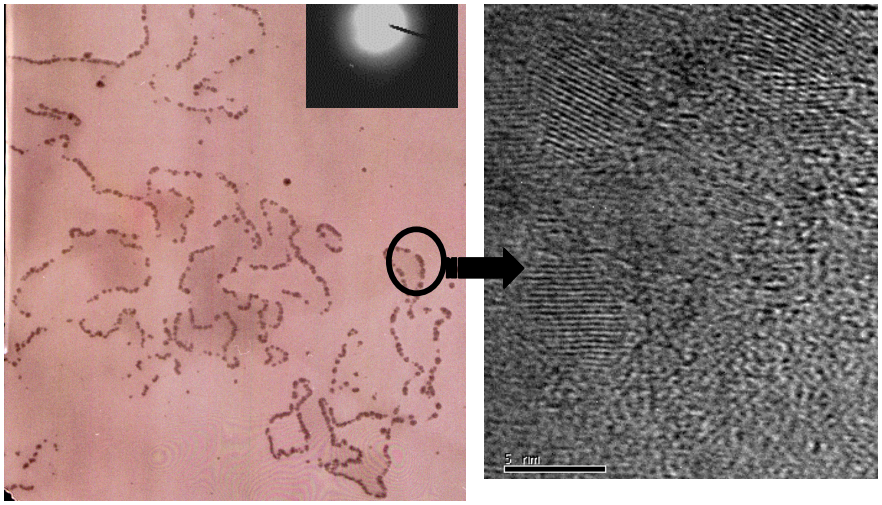

Figure 2 A B
Figure 2 shows (A) low resolution and (B) high resolution lattice TEM images of the phage nanoparticle wires.

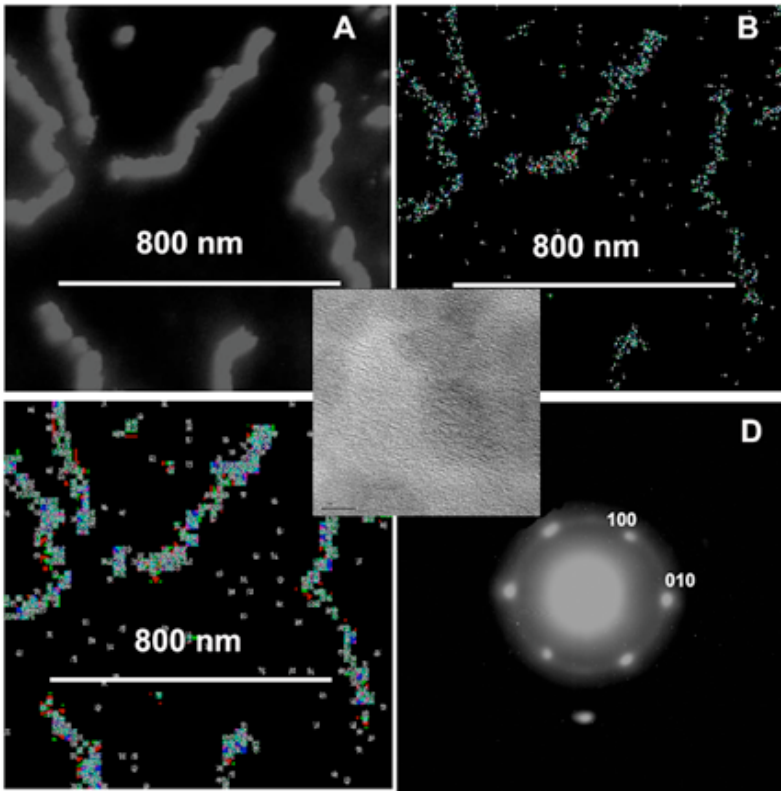

Figure 3. (A) STEM dark field image of A7-P8 phage covered by ZnS nanocrystals. (B) and (C) are corresponding Zn and S mapping. The electron diffraction pattern (D) taken from one phage shows well crystallized wurtzite ZnS nanocrystals were nucleated and aligned along the phage with preferred crystallographic orientation. ZnS Lattice image is center insert

We will continue to explore the use of the phage coat for nucleation of II-VI semiconductor nanoparticles as well as magnetic nanoparticles such as Fe_3O_4 and FePt. A critical part of the analysis will be studying the photoluminescence properties of the nanoparticles.

Assembly and Characterization of Phage Quantum Dot Solids

II-VI semiconductor quantum dots (QDs) (CdSe, CdS, ZnS) exhibit a wide range of electrical and optical properties that are tunable by tailoring the sizes and shapes of the nanocrystals and consequently find potential applications in optoelectronic devices.

Several processes have been developed to prepare QDs. A very successful process is a high temperature (300-360 ºC) organometallic route developed by Bawendi, Alivisatos and their co-workers. This process has recently been shown to be successful for the preparation of magnetic cobalt nanocrystals When QDs are built into close-packed ensembles (QD solids), collective physical phenomena such as the evolution of the localized electron state of an individual QD to a delocalized electronic state will develop as neighboring QDs interact with each other. The inter-dot interactions result in new ensemble physical properties such as long-range resonance transfer of electronic excitations, suppression of non-radiative loss, red shifting and broadening of the optical transition, and electroadsorption response. QD solids have the potential for novel electronic, optical and optoelectronic applications that combine both the collective physical properties of coupled QDs and the unique size-dependent physical properties of individual QDs. Many applications such as the coupled QD quantum computer, wireless interconnects, high optical gain, low threshold current QD lasers and resonant electron tunneling QD devices may result. Consequently, wide interest has been stimulated in the preparation of QD solids (ordered or disordered) by different processes such as photolithography, molecular-beam epitaxy, self-assembly induced by solvent evaporation and templated organization by biomolecules or lyotropic liquid crystals. However, the QD solids prepared by those processes do not contain QDs in close contact and it is difficult to achieve well-defined shapes of QD solids prepared by other methods. Moreover, other synthesis techniques rely on specific substrates/matrix, where the QD solids are not easily transferred.

In my group his year we have developed a new design strategies for the synthesis of QD solids. Our methods utilize cold treatment (-25°C - 85 ºC) for chemical processing of II-VI semiconductor QDs (submitted JACS). Each of these synthesis schemes provides highly reproducible control of particular 3D shape and nanostructure for the QD solids with well-defined size and shape. Using ARO funding we have combined combine our new synthetic route for making quantum dot solids with our phage pVIII synthesis of quantum dot wires to produce phage hybrid quantum solids. Different synthesis routes have been tested as well as different peptide sequences and types of quantum dots. Below, Figure 4, is our first attempt at the "marriage" between our two synthesis methods.

Figure 4 **A** **B** **C**

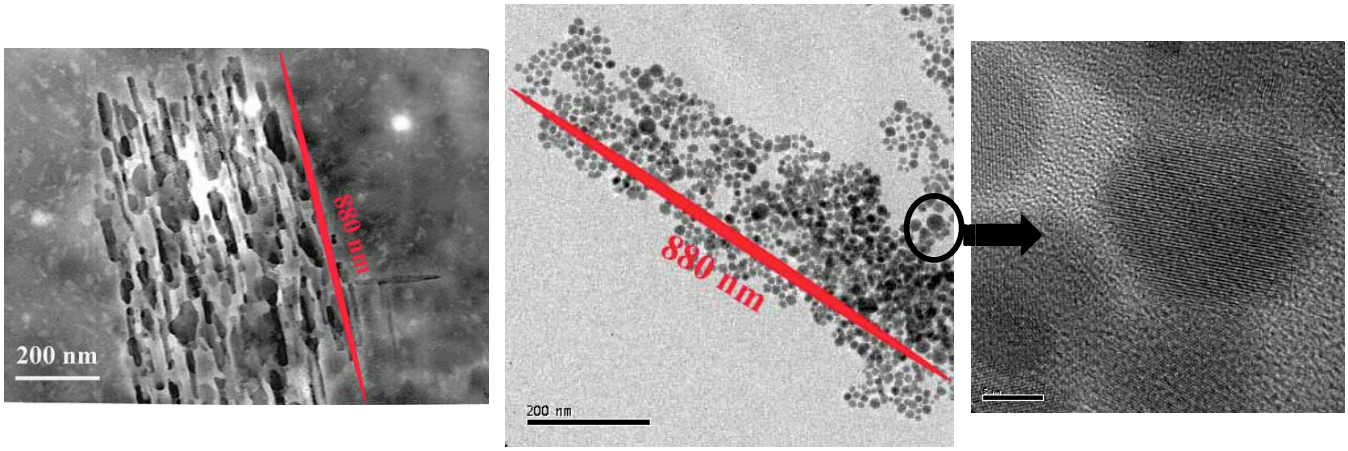

Figure 4 A is a low kV (at 80kV the phage can be imaged intact) TEM image of the aligned phage. Figure 5 B is a 200 kV image of the same region where the quantum dots that are associated with the phage can be seen. Figure 5 C is a high-resolution lattice image of the same region showing the nanoparticles are hexagonal ZnS.

Viral QD Liquid Crystal Films (Science May 3, 2002)

Monodisperse biomaterials that have an anisotropic shape are a promising way to build well-ordered structures. Liquid crystalline structures of wild type viruses (Fd, M13, TMV) were tunable by controlling the solution concentrations, the solution ionic strength, and the external magnetic fields applied to the solutions. We have recently shown that engineered viruses can recognize specific semiconductor surfaces through the selection by combinatorial phage display method. These specific recognition properties of the virus can be used to organize inorganic nanocrystals, forming ordered arrays over the length scale defined by liquid crystal formation. We have evolved phage and ZnS precursor solutions to self-assemble highly oriented, self-supporting films. In this system, we can easily modulate both the length of bacteriophage and the type of inorganic materials through genetic modification and selection. This ARO grant supported our first effort to build multi-length scale ordering of quantum dot (QD) hybrid self-supporting bio-composite structures using genetically engineered M13 bacteriophage, viruses, with monodisperse size and shape. The resulting QD hybrid film material was ordered at the nanoscale and at the micron scale into 72 um domains. These domains repeated continuously over a centimeter length scale. Moreover, viral suspensions containing ZnS QDs were prepared in which the liquid crystalline phase behaviors of the hybrid material were controlled both by the solvent concentration and the use of an applied magnetic field.

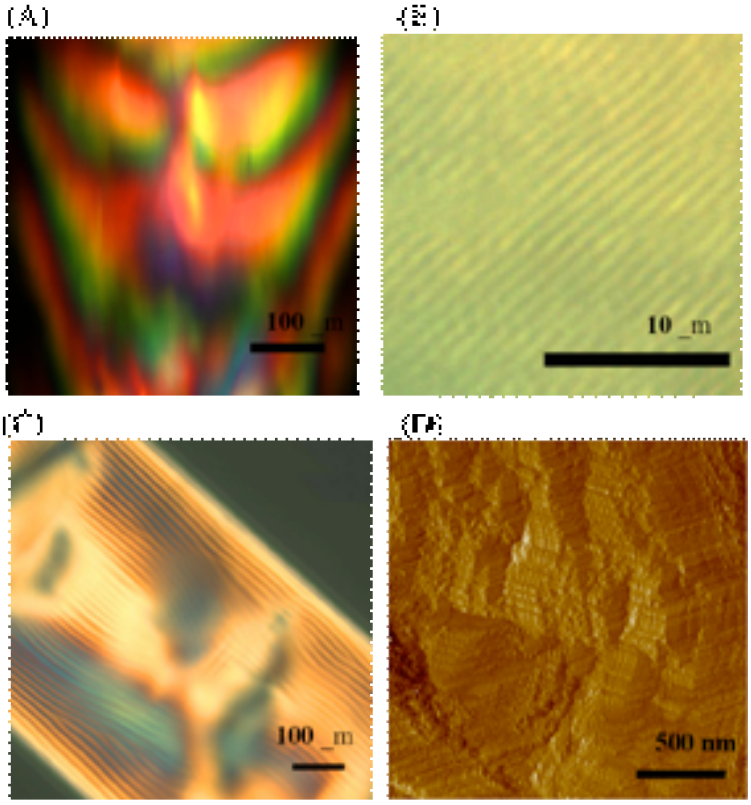

The most dominant selected peptide binding motif with specific recognition to ZnS crystal surfaces was isolated through screening of phage display libraries. The screening method selected for binding affinity of a population of random peptides displayed as part of the pIII minor coat protein of M13. Selected peptides were expressed at one end of the M13 virus. The virus had a filamentous shape (approximately 880 nm in length and 6.6 nm in diameter), with the peptide insert measuring 10 nm in length . The

dominant binding motif that emerged after five rounds of selection was termed A7, with an amino acid insert sequence of CYS-ASN-ASN-PRO-MET-HIS-GLN- ASN-CYS, in which the two cysteine groups formed a disulfide bond, restricting the peptide structure to a constrained loop. The peptide expressed on the virus was tested and confirmed to have binding specificity to ZnS crystal surfaces. The bacteriophage containing this A7 peptide was termed A7 phage, and was cloned and amplified to liquid crystalline concentrations, with DNA verification after each amplification step. See Figure 5.

Figure 5. Characterization of the liquid crystalline suspensions of A7 phage-ZnS nanocrystals and cast film. (A) A polarized optical microscopy (POM) image of a smectic suspension of A7-ZnS at a concentration of (127 mg/ml), (B) a differential interference contrast (DIC) filter brought out ~1 um dark and bright periodic stripes that showed constructive and destructive interference patterns generated from parallel aligned smectic layers in the A7- ZnS suspension, (C) the characteristic fingerprint texture of the cholesteric phase of an A7-ZnS suspension (76 mg/ml), (D) an AFM micrograph of a cast film from an A7 phage-ZnS nanocrystal suspension (~30 mg/ml) showing close-packed structures of the A7 phage particles.

Highly ordered A7 phage-ZnS nanocrystal self-supporting viral films, (Fig. 6A), were prepared from an isotropic phase of bacteriophage and ZnS precursor solutions . The viral nanocrystal hybrid film was transparent and easily manipulated with forceps. Isotropic liquid crystalline phase concentration (~5 mg/ml) was chosen for better ZnS nanocrystal mobility in A7 phage concentrated suspension media, coupling and self-assembly. The films were typically ~15 um thick and several centimeters in extent. The surface viral morphology was smectic O while the interior morphologies were smectic A and C. The ordered-morphologies of the viral film were characterized by POM, scanning electron microscope (SEM), TEM and AFM.

Optical characterization revealed that the films were composed of ~72 um periodic domains that had smectic layer structures within the domain boundaries (Fig. 6B). Using high resolution SEM, the spacing of periodic layers of both the phage and ZnS nanocrystals were apparent. The films showed smectic-like lamellar morphologies between the ZnS nanocrystals and A7 phage layers (Fig. 6G). The periodic length (895 nm) corresponded to that of the bacteriophage (880 nm) and nanocrystal aggregates (~20 nm). The average size of the nanocrystal aggregates in the film was ~20 nm as observed in the TEM of individual virus particles with nanocrystals. Microtomed 50 nm cross sections of a viral film showed 2-3 nm size nanocrystals that were aligned approximately 20 nm in width and extended to more than 2 um in length. The 2 um by 20 nm bands formed in parallel and were separated by ~700 nm. This shorter spacing than expected distance (M13 phage length: 880 nm) corresponds to the length scale imposed by the phage which formed the tilted smectic alignment of the phage with respect to layer normal.

AFM observation of free surface orientation of the A7 phage-ZnS nanocrystal film (Fig. 6F) showed that the phage formed parallel aligned smectic O herringbone patterns. Phage particles had long range orientational ordering that was persistent over many microns. Inorganic ZnS nanocrystals were confined at junction areas where two adjacent lamellar layers met. Fluorescent imaging of the film (Fig. 6C) exhibited a

pattern of ~1 um fluorescent lines, corresponding to the ZnS nanocrystals arranged in the film. In a control viral film, without ZnS crystals, no fluorescence was observed. Because freely suspended liquid crystalline films form highly ordered structures on the free surface due to the surface forces, smectic O herringbone patterns on the film surface might have higher order than the smectic A or smectic C within inner areas in this film. The observed smectic O morphology of the A7-ZnS film is similar to the high ratio rod-coil ($f_{\text{rod-coil}}$ >0.96) block copolymers, which favor the bilayered and interdigitated morphologies. This similarity to A7-ZnS structure ($f_{\text{phage-nanocrystals}}$: ~0.98) strongly suggests that the A7-ZnS might have interdigitated morphology where the director (phage axis) flips by 180° between adjacent A7-ZnS particles in the film. Considering the packing free energy, the interdigitated structure might be the most stable structure for the particles having a larger head (20 nm nanocrystal aggregates) and long-rod tail particles.

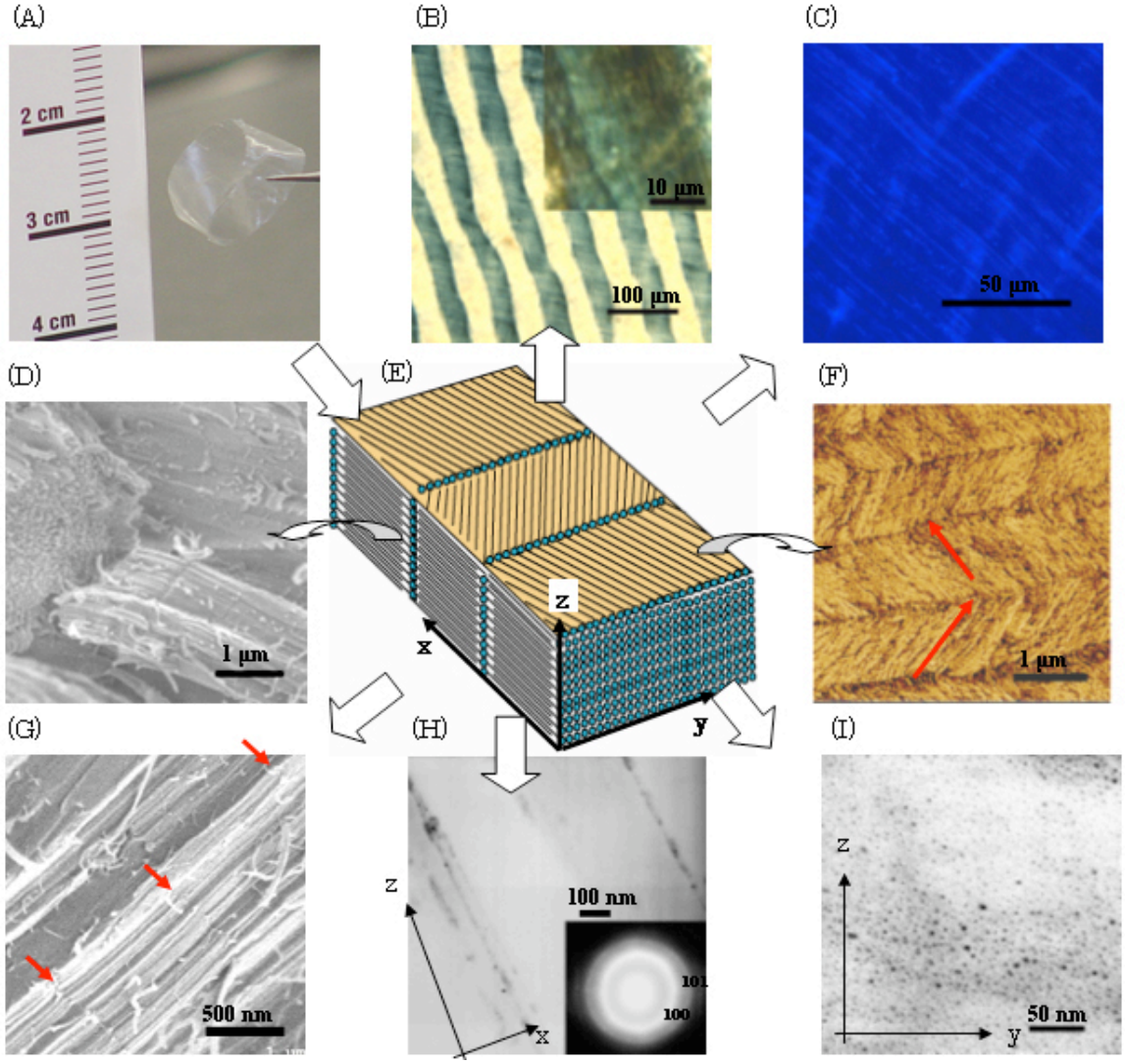

Figure 6. Characterization of A7 phage-ZnS nanocrystal film. (A) A photograph of A7-ZnS viral film, (B) POM (20x) birefringent dark and bright band patterns (periodic length: 72.8 um) were observed. These band patterns are optically active and their

patterns reverse depending on the angles between polarizer and analyzer, (C) photoluminescent image, with an excitation wavelength of 350 nm and with filtering below 400 nm, showed ~1 um stripe patterns (50x), (D) SEM images of highly packed three dimensional bulk film structure, (E) a schematic structural diagram of the A7 phage-ZnS nanocrystal composite film, (F) an AFM image of the free surface showed that the phage formed parallel aligned herringbone patterns that have almost right angles between the adjacent director (red arrows), (G) SEM image that showed the close-packed lamellar structure of phage and nanocrystal layers (red arrows) in the inner areas of the film, (H) low resolution TEM image of cross section of A7 phage-ZnS nanocrystal film with 20 nm x 2 um ZnS nanocrystal stripe pattern aligned between one phage length in the x-z direction of film, and an electron diffraction pattern of ZnS wurtzite structure in inset, and (I) low resolution TEM image of film viewed in the y-z direction showing ZnS nanocrystals.

Viral Films as DNA Storage

In order to fabricate viral films, a phage library that contained 10^9 population of phage were amplified in large volume to get the highly concentrated viral suspension. The viral film was fabricated on the liquid / solid interfaces with gradual decrease of the liquid phase by evaporation of the solvent. As the solvent was gradually removed, the phage particles formed epitaxial layer domains on the surface of a solid substrate. Polarized optical micrograph showed phage layer formed ~ 34 um repeating patterns that continued on the centimeter scale. AFM images showed that the phage particles formed ~500 nm domain where phage particles are laterally stacked relative to each other. These micro-domains are packed to form lamellar like layer in the bulk film.

To test if the viral film can preserve all the phage library clones (both protein and DNA stability) without the loss of the infecting ability, the viral film was re-suspended and used for biopanning a streptavin coated surfaces, which is known to have specific binding motifs (His-Pro-Gln). From the second round sequencing results, His-Pro-Gln sequence appeared at the end of the pIII units. After the fourth round screening, the all peptide sequences showed the consensus to have His-Pro-Gln (Figure 7).

Titer numbers showed that there was little change in the order of the titer number for seven weeks (Table 1). After five months, the titer number was decrease to 10 % of its original concentration.

These biopanning results and infecting ability of the dried phage indicate that the film fabrication using phage library preserves the phage population at room temperature for up to % months. We are currently tested storage for up to 1 year. The film fabrication is a novel process for storage of high density engineered DNA information. Using bacterial hosts, the viral components can be replicated easily at any time. We expect that the viral film will trigger the viral research involved with functionalizing viruses by expressing useful protein units on several different coat proteins, not as a virus, but as a antidotes and vaccines in the future.

Figure 7

3^{TH} ROUND Sequencing Results
LSB-11 TRP ASP PRO TYR SER HIS LEU LEU GLN HIS PRO GLN
LSB-12 ILE GLY SER ARG ALA GLU THR MET PRO TRP PRO ARG

LSB-13 LEU PRO VAL ASN ALA TRP LEU VAL SER HIS PRO GLN
LSB-14 GLN PRO SER TRP SER LEU LEU LEU GLU HIS PRO HIS
LSB-15 GLN PRO SER TRP SER LEU LEU LEU GLU HIS PRO HIS
LSB-16 GLN PRO SER TRP SER LEU LEU LEU GLU HIS PRO HIS
LSB-18 TRP ASP PRO TYR SER HIS LEU LEU GLN HIS PRO GLN
LSB-19 ALA ALA LYS ALA THR LEU SER GLY THR ALA SER VAL
Lsa-1 VAL PRO GLN ILE PRO ASN TRP ILE SER HIS PRO MET
Lsa-2 TRP ASP PRO TYR SER HIS LEU LEU GLN HIS PRO GLN
Lsa-10 TRP ASP PRO TYR SER HIS LEU LEU GLN HIS PRO GLN

4TH ROUND Sequencing Results
*LSA-22 TRP ASP PRO TYR SER HIS LEU LEU GLN HIS PRO GLN
LSA-24 THR THR PHE PRO TRP LEU GLN THR HIS PRO GLN
LSA-25 GLN ASN TRP THR TRP SER LEU PRO HIS HIS PRO GLN
*LSA-26 TRP ASP PRO TYR SER HIS LEU LEU GLN HIS PRO GLN
*LSA-27 TRP ASP PRO TYR SER HIS LEU LEU GLN HIS PRO GLN
*LSA-28 TRP ASP PRO TYR SER HIS LEU LEU GLN HIS PRO GLN
*LSA-29 TRP ASP PRO TYR SER HIS LEU LEU GLN HIS PRO GLN
*LSA-30 TRP ASP PRO TYR SER HIS LEU LEU GLN HIS PRO GLN

Table 1. Time dependence of titer number of biofilm suspended in 1 ml TBS buffer.

Titering date	days	PFU
9/26/01	0	5.1×10^6
9/27/01	1	2.3×10^6
9/29/01	3	2.2×10^6
10/1/01	5	4.7×10^6
10/5/01	9	2.3×10^6
10/11/01	15	1.4×10^6
11/6/01	40	1.0×10^6
11/15/01	49	1.6×10^6
3/7/02	160	2.4×10^5

Toward Developing Hybrid Detector-Antidote Films

Hybrid materials that acts as high-density ultra-small chemical or biological warfare sensors that are also on demand edible or deliverable vaccines and antidotes. High density, transparent, flexible genetically engineered virus crystalline films will be evolved that have already been shown to be stable without solvent for one year without loss of DNA information or proteins structure. Using multiple copies for 7 engineerable proteins these films can carry peptides, proteins and DNA based antidotes and vaccines at

1 X 10 ^{17} antidote copies /cm^3 of film. Part of the viral film will be further evolved to act as a sensor that can detect foreign antigens. Upon detection the film composed of the sensor/antidote complex can be ingested, delivered internally or applied as a patch. These films can also be used for high density storage of genetic information that can be easily recovered on demand.

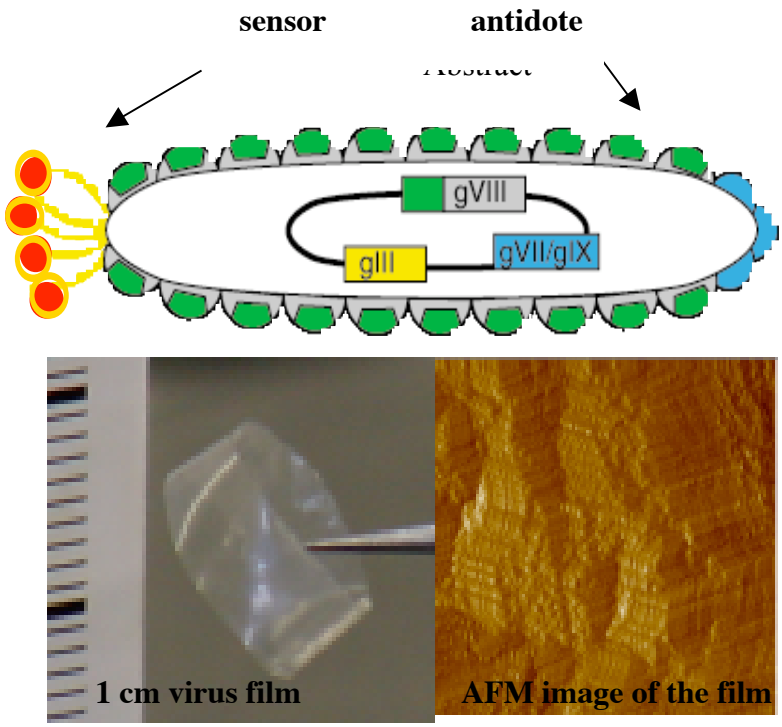

Chiral Smectic C Structures of Virus Based Films (Langmuir in press 2003)

Long-range ordered virus based films were fabricated using M13 phage (viruses) which were aligned and assembled using the meniscus phenomena. Their ordered structures and morphologies were studied and characterized using polarized optical microscopy (POM), atomic force microscopy (AFM) and scanning electron microscopy (SEM). M13 virus particles which are 880 nm in length were the basic building block of the fabricated films. Due to the unique micrometer length scale of viruses, the smectic ordering of virus particles could be easily visualized using conventional microscopy techniques and compared with a theoretical model of chiral liquid crystal structures. From the results of POM, AFM and SEM, the viral films were determined to have a chiral smectic C structure. By comparing ordering of film formation as a function of virus concentration and the formation of bundle-like domain structure found in viral thin films,

a mechanism of film formation is suggested. These virus based film structures are organized on multiple length scales, easily fabricated, and allow integration of aligned semiconductor and magnetic nanocrystals. These self-assembled hybrid materials may have applications in miniaturized self-assembled electronic devices.

Building well ordered and defect-free two- and three-dimensional structures on the nanometer scale has become a critical issue for the construction of next-generation optical, electronic and magnetic materials and devices. Although numerous techniques to organize nanoparticles and other nanometer-sized objects at small-length scales have been attempted, including traditional hydrogen bonding recognition to newly developed DNA linker system, extending such patterns to the micrometer scale has proven difficult. The use of biological materials might provide alternative routes to conventional processing methods for the construction of miniaturized nanoscale devices. Several desirable features of biological systems include the ability to orchestrate precise self assembling structures, highly evolved molecular recognition for both organic and inorganic materials and ability to synthesis inorganic materials into hierarchical structures. Several types of biomaterials have been exploited in the nanoscale assembly of complex architectures. Recently, our group has reported a new method for self-assembling quantum dots in well ordered nanocrystal films using nanocrystal-functionalized M13 phage. M13 viruses were genetically engineered to nucleate or bind desired materials on one-end of the M13 virus. These nanocrystal-functionalized viral liquid crystalline building blocks were grown into hybrid ordered self-supporting films. The resulting nanocrystal hybrid films were ordered at the nanometer scale and at the micrometer scale into 72 _m periodic patterns. We previously reported the smectic O structures on the surfaces and smectic A or C structures in the bulk of the nanocrystal hybrid film.

Here we present more extensive characterization of these virus based films including chiral effects of virus building blocks and provide strong evidence that these virus based films are organized into chiral smectic C structures. The viral films fabricated from different concentrations provide various other textures depending on the thickness of the films. We also compared the viral film results with the ZnS nanocrystal hybrid viral film we previously reported.

We believe this is the first example of a long range ordered lyotropic liquid crystalline chiral smectic C film. This is further evidence that support Meyer's theoretical suggestion that all smectic C structures formed from the chiral molecules should have chiral smectic C structures. Although several microscopy techniques have been used to visualize ordered liquid crystalline materials, understanding of molecular orientation of the liquid crystalline ordered structure has been limited by the small size and softness of the mesogen units of conventional liquid crystalline materials. However, using micrometer scale biomolecules (viruses), surface defects of chiral smectic C structures were easily characterized. Moreover, in order to fabricate defect free and well-ordered complex architectures using virus building block, a basic understanding of the surface and bulk structures of these materials is essential for further application into the semiconductor nanocrystal hybrid virus films.

Virus Based Alignment of Inorganic, Organic, and Biological Nano-sized Materials

(in review Advanced Materials)

Here we present a new platform for organization of a variety of materials including inorganic nanoparticles, small organic molecules and large biomolecules that organize and self-assemble at the nanometer length scale and are continuous into the centimeter length scale. Long-range ordered nano-sized materials (10 nm gold nanoparticles, fluorescein, phycoerythrin protein) were fabricated using a streptavidin linker and anti-streptavidin M13 bacteriophage (virus). The anti-streptavidin viruses, which formed the basis of the self-ordering system, were selected to have a specific recognition moiety for streptavidin using phage display. The nano-sized materials were previously bound to streptavidin. Through the molecular recognition of the genetically selected virus, the nano-size materials were bound and spontaneously evolved into a self-supporting hybrid film.

Functionalized liquid crystalline materials might provide various pathways to build well-ordered and well-controlled two and three-dimensional structures for the construction of next generation optical, electronic and magnetic materials and devices.It has been demonstrated that several types of rod-shape viruses form well controlled liquid crystalline phases. Recently, our group reported a self-assembled ordered nanocrystal film fabrication method using nanocrystal-functionalized M13 virus. Through the utilization of genetic engineering techniques, one-end of the M13 virus was functionalized to nucleate or bind to a desired semiconductor material. These nanocrystal-functionalized viral liquid crystalline building blocks were grown into ordered hybrid self-supporting films. The resulting nanocrystal hybrid film was ordered at the nanoscale and at the micrometer scale into 72 _m periodic striped pattern domains. In the previous system, we could easily nucleate and align the nanoparticles for the II-VI semiconductor materials in an one-pot synthetic route. In order to align other materials including metals and electro-optical materials, biological selection and further evolution are required for each material prior to aligning the nanoparticles. Here we report a novel nanoparticle alignment method using anti-streptavidin viruses, where the virus was first selected to bind streptavidin protein units. This allows a universal handle for the virus to pick up any material that has been covalently conjugated to streptavidin. Then the self assembling nature of this anti-streptavidin virus can be exploited to make organized hybrid materials. The organized hybrid materials presented here are liquid crystalline films of gold nanoparticles, fluorescent molecules (fluorescein) and large fluorescent proteins (phycoerythrin).

The anti-streptavidin M13 viruses having specific binding moieties for the streptavidin were isolated through the screening of a phage display library . Streptavidin has the known specific binding motif His-Pro-Gln. His-Pro-Gln sequences were isolated as pIII inserts after second round selection of phage for the streptavidin target. His-Pro-Gln binding motif made up 100 % of the pIII insert after fourth round selection and sequencing. The dominant binding sequence after the fourth round was TRP ASP PRO TYR SER HIS LEU LEU GLN HIS PRO GLN. This anti-streptavidin M13 virus was amplified to high concentration (~10^{12} pfu) and reacted with 10 nm gold nanocrystals , fluorescein, and phycoerythrin which were previously conjugated with streptavidin. These highly concentrated suspensions exhibited liquid crystalline properties.

2. (6) a. papers in peer review journals:

S.W. Lee, C. Mao, C. Flynn, A. M. Belcher (2002) Ordering of Quantum Dots Using Genetically Engineered Viruses. **Science** 296; 892-895.

N. Seeman and A. M. Belcher (2002) Emulating Biology: Building Nanostructures from the Bottom Up. **PNAS** 10; 1073.

S. W. Lee, B. M. Wood, and A. M. Belcher (2002) Chiral smectic C* structures of viral films **Langmuir**, in press, 2003.

S. R. Whaley, D. S. English, E L. Hu, P. F. Barbara, A. M. Belcher (2000) Biomolecular Recognition and Selection of Peptides for Specific Crystallographic Semiconductor Surfaces. **Nature** 405: 665-668.

S. R. Whaley and A. M. Belcher , Borrowing Ideas from Nature: Peptide Specific Binding to Gallium Arsenide,2000, **MRS Proceedings v. 599, 189-199.**

b. non peer review:

E. E. Gooch and A. M. Belcher, Protein Components and Inorganic Structure in Shell Nacre, in Bio-mineralization of Nano-and Micro-structures, Edmund Baeuerlein ed., **Wiley_VCH,** 2000, 221-248.

c. meeting: at least 25

d. submitted papers:

C. Mao, C. Flynn, A. Hayhurst, R. Sweeney, J. Qi, J. Williams, G. Georgiou, B. Iverson and A. M. Belcher (2002) Viral Assembly of Oriented Quantum Dot Nanowires. **Nature**, In Revision Jan. 2003.

S.W. Lee, S. K. Lee and A. M. Belcher (2002), Virus Based Alignment of Inorganic, Organic, and Biological Nano-sized Materials, Advanced Materials**.**

e. Technical reports : 2 interm reports

2. (7) Advanced Degrees: Sandra Whaley, Christine Flynn

2. (8) Inventions:

Biological Control of Nanoparticle Nucleation, Shape, and Crystal Phase

Nanometer Scale Ordering of Hybrid Materials

High Density Storage of Virus Libraries and Genetic Information as Crystalline Films